Analyst

PAPER

Cite this: *Analyst*, 2015, **140**, 6532

Strand displacement activated peroxidase activity of hemin for fluorescent DNA sensing†

Quanbo Wang,[a] Nan Xu,[a] Zhen Gui,[b] Jianping Lei,[a] Huangxian Ju*[a] and Feng Yan*[b]

Received 16th June 2015,
Accepted 6th August 2015

DOI: 10.1039/c5an01206f

www.rsc.org/analyst

To efficiently regulate the catalytic activity of the peroxidase mimic hemin, this work designs a double-stranded DNA probe containing an intermolecular dimer of hemin, whose peroxidase activity can be activated by a DNA strand displacement reaction. The double-stranded probe is prepared by annealing two strands of hemin labelled DNA oligonucleotides. Using the fluorescent oxidation product of tyramine by H_2O_2 as a tracing molecule, the low peroxidase activity of the hemin dimer ensures a low fluorescence background. The strand displacement reaction of the target DNA dissociates the hemin dimer and thus significantly increases the catalytic activity of hemin to produce a large amount of dityramine for fluorescence signal readout. Based on the strand displacement regulated peroxidase activity, a simple and sensitive homogeneous fluorescent DNA sensing method is proposed. The detection can conveniently be carried out in a 96-well plate within 20 min with a detection limit of 0.18 nM. This method shows high specificity, which can effectively distinguish single-base mismatched DNA from perfectly matched target DNA. The DNA strand displacement regulated catalytic activity of hemin has promising application in the determination of various DNA analytes.

Introduction

Benefitting from the powerful programmable capability, DNA has been assembled into complex three-dimensional structures,[1,2] drug transportable nano-capsules[3,4] or stimuli-responsive hydrogels.[5–7] The DNA-guided assembly of nanomaterials has been used to fabricate three-dimensional nanostructures[8–11] or develop sensors for small molecules and nucleic acids.[12–18] The space distribution of nanomaterials on the DNA templates can be precisely controlled for the design of a signal switch.[19,20] Thus, the DNA-guided assembly of enzymes has become an emerging area.[21–25]

In order to improve the catalytic properties of horseradish peroxidase (HRP), which is extensively utilized in electrochemical, photoelectrochemical or fluorescence sensing,[26–30] DNA nanostructures have been used as a template to assemble enzyme nanocomplexes.[21–25] For instance, assembling HRP and glucose oxidase on a DNA template and then encapsulating them within a thin polymer shell can afford improved catalytic efficiency.[23] As the active cofactor of HRP, hemin is a promising peroxidase mimic.[31–35] Its catalytic activity can be enhanced by the formation of G-quadruplex/hemin DNAzyme,[31–35] or its adsorption on some carbon nanomaterials.[36,37] Our previous work demonstrated the formation of an intramolecular dimer of hemin by labelling two ends of an oligonucleotide with two hemin molecules and proposed a hybridization strategy to regulate the peroxidase activity of hemin for detection of the target DNA.[38] However, the circular probe showed limited ability to distinguish single-base mismatched DNA from perfectly matched target DNA. To address this problem, this work further designs an intermolecular dimer of hemin labelled on two oligonucleotides and introduces DNA strand displacement to achieve the regulation of the peroxidase activity (Scheme 1).

DNA strand displacement can occur when a short single-stranded DNA in a double-stranded DNA complex is displaced by another long single-stranded DNA, usually with the help of a toehold.[39–42] It has been used for biosensing of both nucleic acids and proteins.[43–47] Here the strand displacement with target DNA leads to the dissociation of a double-stranded DNA probe (Scheme 1A). The probe was prepared with two pieces of hemin labelled ssDNA. The neighbouring two hemin molecules on the double-stranded probe formed a hemin dimer with low peroxidase activity. After the strand displacement with target DNA, two pieces of hemin labelled ssDNA were separated to dissociate the hemin dimer and form highly active hemin monomers. Using the oxidation reaction of

[a]*State Key Laboratory of Analytical Chemistry for Life Science, School of Chemistry and Chemical Engineering, Nanjing University, Nanjing 210093, P.R. China. E-mail: hxju@nju.edu.cn; Fax: +86 25 83593593; Tel: +86 25 83593593*

[b]*Department of Clinical Laboratory, Nanjing Medical University Cancer Hospital & Jiangsu Cancer Hospital, 42 Baiziting Road, Nanjing 210009, P.R. China. E-mail: yanfeng2007@sohu.com*

†Electronic supplementary information (ESI) available. See DOI: 10.1039/c5an01206f

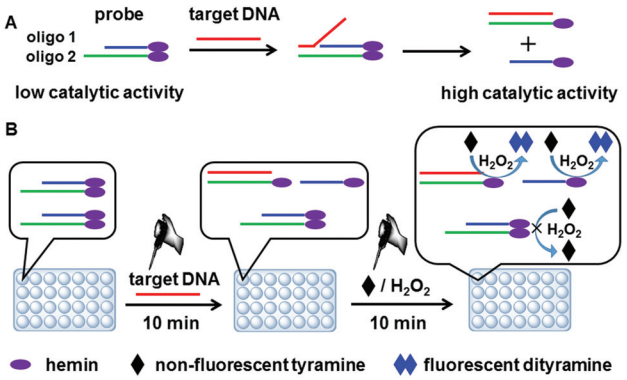

Scheme 1 Schematic illustration of (A) target DNA-strand displacement reaction regulated catalytic activity of the double-stranded probe, and (B) homogeneous fluorescence strategy for DNA sensing in a 96-well plate.

non-fluorescent tyramine by hydrogen peroxide (H_2O_2) as a model, the total signal derived from the enzymatic catalysis of hemin produced fluorescent dityramine (Scheme S1, ESI†). The reaction possessed quick dynamics and could be completed within 10 min, leading to a relatively fast fluorescence method for target DNA detection (Scheme 1B). The detection of DNA could be conveniently carried out in a 96-well plate with high specificity and high-throughput, indicating its promising applicability in complex samples.

Experimental

Materials and reagents

Tyramine and tris(hydroxymethyl) aminomethane (tris) were purchased from Sigma–Aldrich Inc. (USA). Opti-MEM reduced-serum medium (Item no. 31985-070) was obtained from Thermo Fisher Scientific (USA). Tris-HCl buffer (50 mM, containing 200 mM NaCl, pH 7.4) was used for homogeneous fluorescence measurements. All other reagents were of analytical grade and used without further purification. Ultrapure water obtained from a Millipore water purification system (≥18 MΩ, Milli-Q, Millipore) was used in all assays. All oligonucleotides were synthesized and purified using high-performance liquid chromatography by TAKARA Biotechnology (Dalian, China), and their sequences are listed below:

Oligonucleotide 1 (oligo 1): 5′-GTCTGTTTGAGGTTGCT-hemin-3′
oligo 2: 5′-hemin-AGCAACCTCAAACAGACACCATGG-3′
oligo 3: 5′-GGTGTCTGTTTGAGGTTGCT-hemin-3′
oligo 4: 5′-GTGTCTGTTTGAGGTTGCT-hemin-3′
oligo 5: 5′-TGTCTGTTTGAGGTTGCT-hemin-3′
oligo 6: 5′-TCTGTTTGAGGTTGCT-hemin-3′
oligo 7: 5′-CTGTTTGAGGTTGCT-hemin-3′
oligo 8: 5′-TGTTTGAGGTTGCT-hemin-3′
oligo 9: 5′-GTTTGAGGTTGCT-hemin-3′
Target DNA: 5′-CCATGGTGTCTGTTTGAGGTTGCT-3′
Single-base mismatched target 1 (smT1): 5′-CCATGGTGTCTCTTTGAGGTTGCT-3′
smT2: 5′-CCATCGTGTCTGTTTGAGGTTGCT-3′
smT3: 5′-CCATGGTCTCTGTTTGAGGTTGCT-3′
smT4: 5′-CCATGGTGTCTGTTTCAGGTTGCT-3′
smT5: 5′-CCATGGTGTCTGTTTGACGTTGCT-3′
smT6: 5′-CCATGGTGTCTGTTTGAGGTTCCT-3′

Here, oligo 1 and oligos 3–9 were labelled with hemin at their 3′ ends, while oligo 2 was labelled with hemin at its 5′ end. Oligos 1–9 were characterized by mass spectroscopy (Fig. S1–9, ESI†). Single-base mismatched targets with different mismatched positions were named smT1–6, and mismatched bases are highlighted in underlined letters.

Instrumentation

Fluorescence data were recorded on a Varioskan Flash multimode reader (Thermo Scientific, USA). To measure the fluorescence signal of dityramine, the excitation and emission wavelengths were set to 320 and 410 nm, respectively, and the excitation bandwidth was set to 5 nm. UV-vis absorption spectra were obtained with a UV-3600 UV-vis-NIR spectrophotometer (Shimadzu, Japan). Mass spectra were recorded on an Autoflex III Smartbeam mass spectrometer (Bruker, Germany).

Preparation of the double-stranded probe

Firstly, a 200 μL mixture containing oligo 1 (21 μM) and oligo 2 (21 μM) in 50 mM Tris-HCl buffer (pH 7.4, containing 100 mM NaCl) was heated at 90 °C for 10 min, and gradually cooled down to room temperature. The prepared double-stranded probe was then diluted with 50 mM Tris-HCl buffer (pH 7.4, containing 100 mM NaCl) to the concentration of 1 μM and stored at 4 °C before use.

Optimization of detection conditions

A series of Tris-HCl buffers (50 mM) containing 100 mM NaCl were prepared at pH 6.5, 7.0, 7.4, 8.0, 8.5 and 9.0 to optimize the detection buffer, while the buffers (50 mM, pH 7.4) containing different concentrations of NaCl were prepared to optimize the NaCl concentration. The fluorescence signals were recorded after adding 0.7 mM tyramine and 2.0 mM H_2O_2 to 10 nM double-stranded probe in the presence and absence of 10 nM target DNA for 10 min. The maximum ratio of signal to background was examined.

Similarly, 0.18, 0.35, 0.7, 1.4 or 2.8 mM of tyramine and 2.0 mM H_2O_2 were added to the solution of 10 nM double-stranded probe in the presence and absence of 10 nM target DNA, and the fluorescence signals were recorded after a 10 min catalytic reaction to optimize the tyramine concentration. The optimization of H_2O_2 concentration was carried out in a similar method.

Homogeneous fluorescence detection of DNA

In a 96-well plate, after 198 μL mixture of the double-stranded probe (10.1 nM) and target DNA was incubated in 50 mM Tris-HCl buffer (pH 7.4, containing 200 mM NaCl) at room temperature for 10 min, 1.0 μL tyramine (140 mM) and 1.0 μL H_2O_2

(400 mM) were added to initiate the catalytic reaction for 10 min. Finally, the fluorescence emission data at 410 nm were recorded by using a plate reader at an excitation wavelength of 320 nm.

Results and discussion

Structural change of the probe upon recognition of the target

To investigate the dissociation of the hemin dimer upon the recognition of target DNA by the probe, UV-visible absorption spectra of the probe in the absence or presence of the target were obtained. The absorption spectrum of the double-stranded probe showed a broadened peak at 378 nm (Fig. 1A, curve a), which could be attributed to the formation of a face-to-face hemin dimer.[36] After mixing 1 μM double-stranded probe with 1 μM target DNA to incubate for 10 min, the spectrum showed a sharp and red-shifted peak at 402 nm (Fig. 1A, curve b), which was the characteristic peak of the hemin monomer.[36] After being mixed with target DNA, the absorbance of the double-stranded probe at 402 nm increased and reached a plateau at 10 min (Fig. S10, curve blue, ESI†), indicating that the dissociation of the hemin dimer could be completed within 10 min. The change of hemin absorption suggested that the target DNA could displace the oligo 1 on the double-stranded probe, and thus dissociate the hemin dimer on the probe to hemin monomers.

Peroxidase activity change of the probe upon recognition to target

The fluorescence of dityramine was used to trace the change of peroxidase activity of the double-stranded probe upon its recognition to target DNA. The fluorescence spectra were recorded after mixing tyramine (0.7 mM) and H_2O_2 (2.0 mM) with the probe or the mixture of the probe and the target to initiate the catalytic reaction for 10 min. In the absence of target DNA, the fluorescence spectrum of the mixture of tyramine and H_2O_2 with 10 nM probe showed a low fluorescence peak at 410 nm (Fig. 1B, curve a), which could be attributed to the weak catalytic activity of the hemin dimer to produce a small quantity of dityramine. After tyramine and H_2O_2 were mixed with the mixture of 10 nM probe and 10 nM target DNA for 10 min, the fluorescence peak sharply increased (Fig. 1B, curve b), indicating the high peroxidase activity of the hemin monomers on oligo 1 and oligo 2/target duplex due to the dissociation of the hemin dimer after the strand displacement reaction of the probe with target DNA. However, when using 10 nM single-base mismatched target (smT1) to replace perfectly matched target DNA, the fluorescence peak was far below that in the presence of target DNA (Fig. 1B, curve c). Thus the double-stranded probe could effectively distinguish the target DNA and single-base mismatched target,[43–45] which could be used to develop a highly specific DNA detection method.

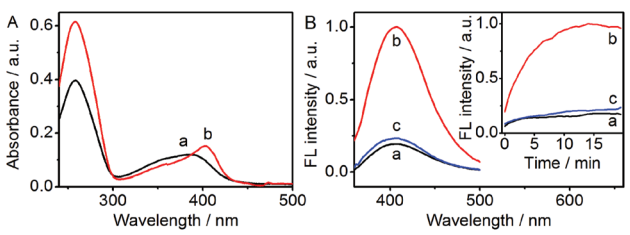

Fig. 1 (A) UV-visible spectra of 1 μM double-stranded probe in the absence (a) and the presence (b) of 1 μM target DNA. (B) Fluorescence spectra of a mixture of 0.7 mM tyramine, and 2.0 mM H_2O_2 with 10 nM double-stranded probe in the absence (a) and the presence (b) of 10 nM target DNA or in the presence of 10 nM smT1 (c). Inset: fluorescence kinetic curves of tyramine oxidation catalysed by the reaction product of 10 nM double-stranded probe without (a) and with (b) 10 nM target DNA or smT1 (c).

As mentioned above, the hemin dimer showed weak catalytic activity, thus the fluorescence signal of the mixture of tyramine (0.7 mM), H_2O_2 (2.0 mM) and the double-stranded probe (10 nM) showed a slightly increased fluorescence signal at 410 nm over time (Fig. 1B inset, curve a). After hybridizing 10 nM double-stranded probe with 10 nM target DNA for 10 min, the fluorescence signal of a mixture of 0.7 mM tyramine and 2.0 mM H_2O_2 with the hybridization product at the same reaction time increased obviously (inset in Fig. 1B, curve b). The time-dependent curve gradually reached a plateau at 10 min, indicating a relatively fast enzymatic reaction kinetics. The fluorescence signal of the mixture of tyramine and H_2O_2 with the hybridization product of the double-stranded probe with smT1 (inset in Fig. 1B, curve c) only showed a minor increment compared with the fluorescence signal in the absence of the target, indicating excellent specificity of the double-stranded probe.

Optimization of toehold length

The toehold length of the double-stranded probe in the strand displacement reaction greatly influenced both the strand displacement efficiency and the specificity of the probe. A series of double-stranded probes with different toehold lengths were prepared by hybridizing oligo 1 with hemin-labelled ssDNA (oligo 2–9). Fig. 2 compares the fluorescence signals of the hybridization products of probes with target DNA or smT1 in the presence of H_2O_2 and tyramine. The toehold length showed a negligible effect on the signal catalyzed by the double-stranded probe in the absence of the target (Fig. 2, green). However, with the increasing toehold length from 4 to 11 nt, the fluorescence signal in the presence of target DNA increased gradually and reached a plateau at 7 nt (Fig. 2, red), indicating an increased strand displacement efficiency to produce highly active hemin monomers. Absorbance kinetic curves at 402 nm also suggested that the rate of the strand displacement reaction increased with the elongation of the toehold length, and a toehold length of 7 nt was adequate to fully dissociate the hemin dimer to its monomers in 10 min (Fig. S10, ESI†). In the presence of smT1, the fluorescence signals did not obviously increase until the toehold length reached 8 nt (Fig. 2, blue), which could be attributed to the fact that the long toehold on the double-stranded probe reduced the specificity of the strand displacement reaction.

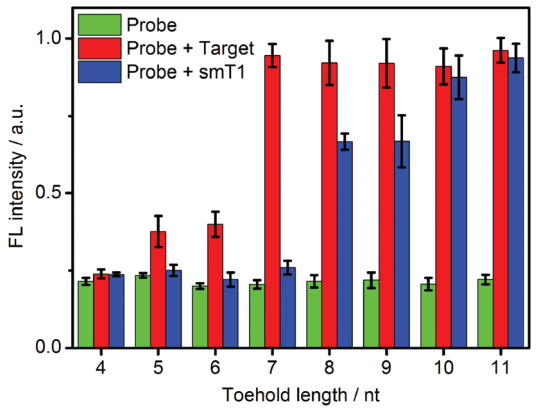

Fig. 2 Effect of the toehold length on the fluorescence signal of dityramine formed in the presence of 10 nM double-stranded probe without (green) and with (red) 10 nM target DNA or 10 nM smT1 (blue).

Thus an optimized toehold length of 7 nt was selected for further experiments, at which the double-stranded probe could be displaced by target DNA with high efficiency, and also effectively discriminate smT1 from perfectly matched target DNA. Notably, the optimized toehold length was a little longer than the previously reported toehold-mediated stand displacement reaction,[41] which could be attributed to the strong face-to-face π–π interaction of the hemin dimer on the double-stranded probe.

Optimization of detection conditions

The ratio of catalytic fluorescence signals of 10 nM double-stranded probe in the presence or absence of 10 nM target DNA was used to optimize the detection conditions (Fig. 3). The pH and ion strength of reaction buffer influenced both the strand displacement and enzymatic reaction rates. Similar to our previous research, high NaCl concentrations decreased the fluorescence signal due to the inhibited peroxidase activity of hemin.[48] The optimal pH and NaCl concentration were 7.4 and 200 mM, respectively (Fig. 3A and B). At 2.0 mM H_2O_2, the ratio increased with the increasing tyramine concentration and reached the maximum value at 0.7 mM (Fig. 3C). A higher concentration of tyramine led to a high fluorescence background and a decreased ratio. Thus 0.7 mM tyramine was used as the optimal condition, at which the maximum ratio occurred at the H_2O_2 concentration of 2.0 mM (Fig. 3D).

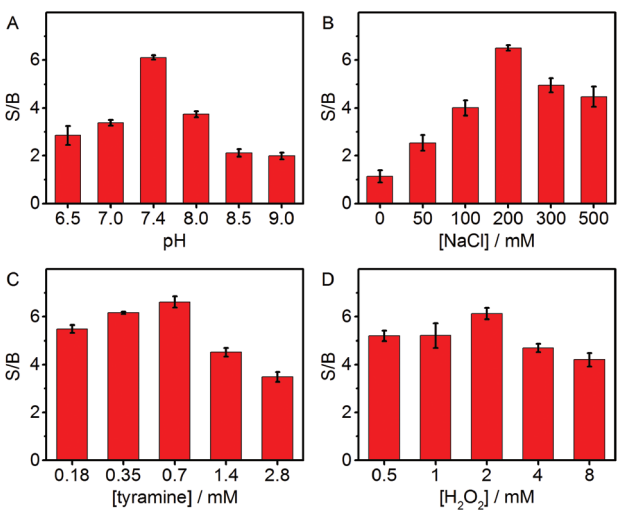

Fig. 3 Effects of (A) pH, (B) NaCl, (C) tyramine and (D) H_2O_2 concentrations on S/B, where S and B are fluorescence signals of the mixtures of 0.7 mM tyramine, 2.0 mM H_2O_2 with 10 nM double-stranded probe in the presence and the absence of 10 nM target DNA, respectively.

Detection of target DNA

The peroxidase activity change of hemin upon the recognition of the double-stranded probe with target DNA to dissociate the hemin dimer offered a method for homogeneous fluorescence detection of DNA. The FL intensity was proportional to the DNA concentration ranging from 0.25 to 10 nM (R = 0.995) (Fig. 4A). The detection limit was estimated at 3σ to be 0.18 nM. The standard deviations for detection of six parallel target DNA samples at 1.0, 5.0 and 10 nM are 4.8%, 7.2% and 1.5%, respectively, indicating the acceptable reproducibility of the proposed method. Compared with previously reported DNA detection methods based on the G-quadruplex/hemin DNAzyme,[33–35] this method showed a lower detection limit and much shorter detection time (Table S1, ESI†). The usage of a plate reader to obtain the detection signal greatly simplified the sensing procedure and improved the detection throughput.

Specificity of the detection method

The specificity of this protocol was investigated by comparing the FL intensity increment in the presence of target DNA or single-base mismatched targets with different mismatch positions (smT1–6). The FL intensity increment in the presence of the single-base mismatched targets was much lower than that of target DNA even in the 10-fold smT concentration (Fig. 4B), indicating excellent specificity of this DNA detection method. The specificity of this method was also examined by changing

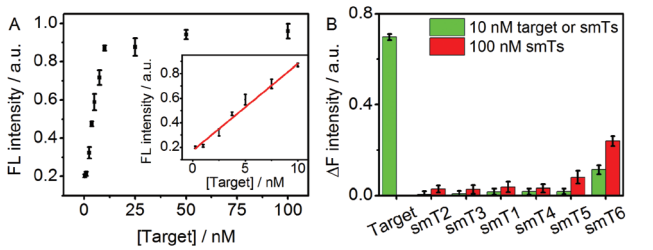

Fig. 4 (A) Fluorescence signals of dityramine formed in the presence of 10 nM double-stranded probe at 0.25, 1.0, 2.5, 3.8, 5.0, 7.5, 10, 25, 50 and 100 nM target DNA. Inset: calibration curve. (B) Fluorescence intensity increment (ΔF) of 10 nM double-stranded probe with 10 nM complementary target or 10 nM (green) and 100 nM (red) single-base mismatched targets (smT1–6).

the mismatch position. The lowest specificity was obtained with smT6 on which the mismatch position was far away from the region complementary to the toehold of the double-stranded probe. This could be attributed to the fact that the mismatch position on the smT6 showed low influence on the strand displacement reaction. Compared to the limited specificity of our previously reported circular probe,[38] the introduction of DNA strand displacement in the probe design greatly improved the specificity for single-base mismatched targets.

Detection of target DNA in cell medium

The feasibility of this method for the detection of target DNA was verified with a cell medium. As supplemented in Fig. S11,† in 100-fold dilution of the cell medium containing 10 nM target DNA, this method showed a comparable response to that in Tris-HCl buffer. The recovery of the detection was calculated to be 103.4 ± 2.3%. These results indicated the potential application of this method for the detection of DNA in complex samples.

Conclusions

This work designed an intermolecular dimer of hemin and a method to effectively regulate the catalytic activity of the HRP mimic hemin by a DNA strand displacement. The low peroxidase activity of the hemin dimer formed on the double-stranded probe ensured a low fluorescence background. The strand displacement reaction of target DNA dissociated the hemin dimer and thus significantly increased the catalytic activity of hemin to produce a fluorescence signal. Based on the strand displacement regulated peroxidase activity, a simple and sensitive homogeneous fluorescence DNA sensing method was proposed. This method showed high specificity, which could effectively distinguish single-base mismatched targets from perfectly matched target DNA. This work paved a promising way for tuning the catalytic activity of natural enzyme mimics by designing switchable DNA structures. Also, the double-stranded probe could be conveniently extended to detect other analytes such as proteins after some modification.

Acknowledgements

This research was financially supported by the National Basic Research Program of China (2010CB732400), the National Natural Science Foundation of China (21135002, 21121091, 21475063), the Leading Medical Talents Program from the Department of Health of Jiangsu Province, and the Science Foundation of Jiangsu (BL2013036).

References

1 B. Wei, M. J. Dai and P. Yin, *Nature*, 2012, **485**, 623–626.
2 Y. G. Ke, L. L. Ong, W. M. Shih and P. Yin, *Science*, 2012, **338**, 1177–1183.
3 S. M. Douglas, I. Bachelet and G. M. Church, *Science*, 2012, **335**, 831–834.
4 H. Lee, A. K. R. Lytton-Jean, Y. Chen, K. T. Love, A. I. Park, E. D. Karagiannis, A. Sehgal, W. Querbes, C. S. Zurenko, M. Jayaraman, C. G. Peng, K. Charisse, A. Borodovsky, M. Manoharan, J. S. Donahoe, J. Truelove, M. Nahrendorf, R. Langer and D. G. Anderson, *Nat. Nanotechnol.*, 2012, **7**, 389–393.
5 H. H. Yang, H. P. Liu, H. Z. Kang and W. H. Tan, *J. Am. Chem. Soc.*, 2008, **130**, 6320–6321.
6 E. J. Cheng, Y. Z. Xing, P. Chen, Y. Yang, Y. W. Sun, D. J. Zhou, L. J. Xu, Q. H. Fan and D. S. Liu, *Angew. Chem., Int. Ed.*, 2009, **48**, 7660–7663.
7 Y. Z. Xing, E. J. Cheng, Y. Yang, P. Chen, T. Zhang, Y. W. Sun, Z. Q. Yang and D. S. Liu, *Adv. Mater.*, 2011, **23**, 1117–1121.
8 A. Kuzyk, R. Schreiber, Z. Y. Fan, G. Pardatscher, E.-M. Roller, A. Hogele, F. C. Simmel, A. O. Govorov and T. Liedl, *Nature*, 2012, **483**, 311–314.
9 X. B. Shen, C. Song, J. Y. Wang, D. W. Shi, Z. G. Wang, N. Liu and B. Q. Ding, *J. Am. Chem. Soc.*, 2012, **134**, 146–149.
10 J.-H. Lee, G.-H. Kim and J.-M. Nam, *J. Am. Chem. Soc.*, 2012, **134**, 5456–5459.
11 Y. X. Xu, Q. Wu, Y. Q. Sun, H. Bai and G. Q. Shi, *ACS Nano*, 2010, **4**, 7358–7362.
12 J. W. Liu and Y. Lu, *J. Am. Chem. Soc.*, 2003, **125**, 6642–6643.
13 J. W. Liu and Y. Lu, *Angew. Chem., Int. Ed.*, 2006, **45**, 90–94.
14 W. Xu, X. Xue, T. Li, H. Zeng and X. Liu, *Angew. Chem., Int. Ed.*, 2009, **48**, 6849–6852.
15 W. Ma, H. Kuang, L. G. Xu, L. Ding, C. L. Xu, L. B. Wang and N. A. Kotov, *Nat. Commun.*, 2013, **4**, 2689.
16 L. H. Guo, Y. Xu, A. R. Ferhan, G. N. Chen and D.-H. Kim, *J. Am. Chem. Soc.*, 2013, **135**, 12338–12345.
17 L. H. Tang, Y. Wang, Y. Liu and J. H. Li, *ACS Nano*, 2011, **5**, 3817–3822.
18 D. C. Leslie, J. Y. Li, B. C. Strachan, M. R. Begley, D. Finkler, L. A. L. Bazydlo, N. S. Barker, D. M. Haverstick, M. Utz and J. P. Landers, *J. Am. Chem. Soc.*, 2012, **134**, 5689–5696.
19 C. S. Yun, A. Javier, T. Jennings, M. Fisher, S. Hira, S. Peterson, B. Hopkins, N. O. Reich and G. F. Strouse, *J. Am. Chem. Soc.*, 2005, **127**, 3115–3119.
20 S. A. E. Marras, F. R. Kramer and S. Tyagi, *Nucleic Acids Res.*, 2002, **30**, e122.
21 R. Freeman, E. Sharon, R. Tel-Vered and I. Willner, *J. Am. Chem. Soc.*, 2009, **131**, 5028–5029.
22 J. L. Fu, M. H. Liu, Y. Liu, N. W. Woodbury and H. Yan, *J. Am. Chem. Soc.*, 2012, **134**, 5516–5519.
23 Y. Liu, J. J. Du, M. Yan, M. Y. Lau, J. Hu, H. Han, O. O. Yang, S. Liang, W. Wei, H. Wang, J. M. Li, X. Y. Zhu, L. Q. Shi, W. Chen, C. Ji and Y. F. Lu, *Nat. Nanotechnol.*, 2013, **8**, 187–192.
24 M. H. Liu, J. L. Fu, C. Hejesen, Y. H. Yang, N. W. Woodbury, K. Gothelf, Y. Liu and H. Yan, *Nat. Commun.*, 2013, **4**, 2127.

25 J. L. Fu, Y. R. Yang, A. Johnson-Buck, M. H. Liu, Y. Liu, N. G. Walter, N. W. Woodbury and H. Yan, *Nat. Nanotechnol.*, 2014, **9**, 531–536.
26 G. Liu, Y. Wan, V. Gau, J. Zhang, L. H. Wang, S. P. Song and C. H. Fan, *J. Am. Chem. Soc.*, 2008, **130**, 6820–6825.
27 Y. L. Wen, H. Pei, Y. Wan, Y. Su, Q. Huang, S. P. Song and C. H. Fan, *Anal. Chem.*, 2011, **83**, 7418–7423.
28 D. Du, L. M. Wang, Y. Y. Shao, J. Wang, M. H. Engelhard and Y. H. Lin, *Anal. Chem.*, 2011, **83**, 746–752.
29 W. W. Zhao, X. Y. Dong, J. Wang, F. Y. Kong, J. J. Xu and H. Y. Chen, *Chem. Commun.*, 2012, **48**, 5253–5255.
30 S. Y. Niu, Y. Jiang and S. S. Zhang, *Chem. Commun.*, 2010, **46**, 3089–3091.
31 P. Travascio, Y. F. Li and D. Sen, *Chem. Biol.*, 1998, **5**, 505–517.
32 D. Sen and L. C. H. Poon, *Crit. Rev. Biochem. Mol. Biol.*, 2011, **46**, 478–492.
33 E. Golub, R. Freeman, A. Niazov and I. Willner, *Analyst*, 2011, **136**, 4397–4401.
34 V. Pavlov, Y. Xiao, R. Gill, A. Dishon, M. Kotler and I. Willner, *Anal. Chem.*, 2004, **76**, 2152–2156.
35 Y. Xiao, V. Pavlov, T. Niazov, A. Dishon, M. Kotler and I. Willner, *J. Am. Chem. Soc.*, 2004, **126**, 7430–7431.
36 T. Xue, S. Jiang, Y. Q. Qu, Q. Su, R. Cheng, S. Dubin, C.-Y. Chiu, R. Kaner, Y. Huang and X. F. Duan, *Angew. Chem., Int. Ed.*, 2012, **51**, 3822–3825.
37 Y. L. Zhou, M. Wang, Z. N. Xu, C. L. Ni, H. S. Yin and S. Y. Ai, *Biosens. Bioelectron.*, 2014, **54**, 244–250.
38 Q. B. Wang, N. Xu, Z. Gui, J. P. Lei, H. X. Ju and F. Yan, *Chem. Commun.*, 2014, **50**, 15362–15365.
39 R. M. Dirks and N. A. Pierce, *Proc. Natl. Acad. Sci. U. S. A.*, 2004, **101**, 15275–15278.
40 D. Y. Zhang, A. J. Turberfield, B. Yurke and E. Winfree, *Science*, 2007, **318**, 1121–1125.
41 D. Y. Zhang and E. Winfree, *J. Am. Chem. Soc.*, 2009, **131**, 17303–17314.
42 W. Tang, H. M. Wang, D. Z. Wang, Y. Zhao, N. Li and F. Liu, *J. Am. Chem. Soc.*, 2013, **135**, 13628–13631.
43 Q. G. Li, G. Y. Luan, Q. P. Guo and J. X. Liang, *Nucleic Acids Res.*, 2002, **30**, e5.
44 T. J. Song and H. J. Liang, *J. Am. Chem. Soc.*, 2012, **134**, 10803–10806.
45 D. Z. Wang, W. Tang, X. J. Wu, X. Y. Wang, G. J. Chen, Q. Chen, N. Li and F. Liu, *Anal. Chem.*, 2012, **84**, 7008–7014.
46 A. X. Zheng, J. Li, J. R. Wang, X. R. Song, G. N. Chen and H. H. Yang, *Chem. Commun.*, 2012, **48**, 3112–3114.
47 F. Li, H. Q. Zhang, Z. X. Wang, X. K. Li, X. F. Li and X. C. Le, *J. Am. Chem. Soc.*, 2013, **135**, 2443–2446.
48 Q. B. Wang, N. Xu, J. P. Lei and H. X. Ju, *Chem. Commun.*, 2014, **50**, 6714–6717.